

# General Methodology of Using Oil-in-Water and Water-in-Oil Emulsions for Coiling Nanofilaments

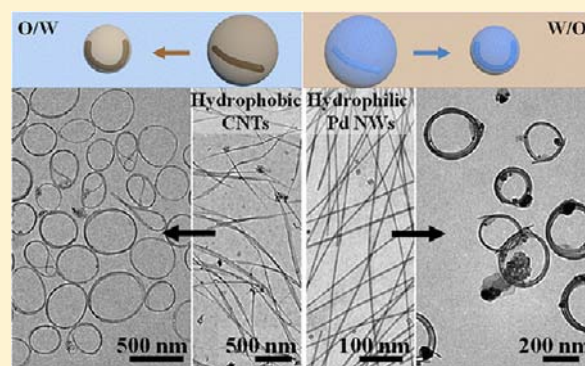
Liyong Chen,<sup>†</sup> Suzhu Yu,<sup>‡</sup> Hong Wang,<sup>†</sup> Jun Xu,<sup>†</sup> Cuicui Liu,<sup>†</sup> Wen Han Chong,<sup>†</sup> and Hongyu Chen<sup>\*†</sup>

<sup>†</sup>Division of Chemistry and Biological Chemistry, Nanyang Technological University, Singapore 637371

<sup>‡</sup>Singapore Institute of Manufacturing Technology, 71 Nanyang Drive, Singapore 638075

**S** Supporting Information

**ABSTRACT:** Hydrophobic carbon nanotubes (CNTs) and hydrophilic nanofilaments such as oxidized CNTs, Pd nanowires (NWs), and MnO<sub>2</sub> NWs are transformed from wires to rings by a general methodology. We show that both oil-in-water and water-in-oil emulsions, so long as their droplet size is sufficiently small, can exert significant force to the entrapped nanostructures, causing their deformation. This effect can be easily achieved by simply mixing a few solutions in correct ratios. Even preformed oil droplets can take in CNTs from the aqueous solution converting them into rings, indicating the important role of thermodynamics: The question here is not if the droplets can exert sufficient force to bend the nanofilaments, because their random vibration may be already doing it. As long as the difference in solvation energy is large enough for a nanofilament, it would “want” to move away from the bulk solution and fit inside tiny droplets, even at the cost of induced strain energy. That said, the specific interactions between a droplet and a filament are also of importance. For example, when an oil droplet rapidly shrinks in size, it can compress the entrapped CNTs in multiple stages into structures with higher curvatures (thus higher strain) than that of a circular ring, which has minimal induced strain inside a spherical droplet.



## INTRODUCTION

Rational design and synthesis of complex nanostructures with precise control<sup>1</sup> is essential for fabricating advanced nanodevices in the future.<sup>2</sup> Such a synthetic advancement requires a fundamental understanding of the underlying processes. The main challenges lie in the difficulty in precisely acting on a nanostructure and in the fact that nanostructures are simply too many to be processed individually.<sup>3</sup>

In the past few decades, chemical synthesis and growth of nanocrystals have been extensively studied.<sup>4</sup> In contrast, there are only limited works on altering the shape of preformed nanostructures.<sup>5,6</sup> To this end, it is difficult to work with objects suspended in a homogeneous solution. With few exceptions,<sup>4a</sup> something (e.g., a tip or membrane) has to interact with them and exert anisotropic force.<sup>5a,7</sup> In fact, one cannot “touch” them without similarly sized objects or interfaces.<sup>8</sup>

An emulsion is a suspension of liquid droplets in another immiscible liquid (Figure 1). An important quality of emulsion is that it can be readily prepared in large scales. Thus, the interface of the two liquids could provide a means to manipulate a large number of colloidal nanostructures. Indeed, emulsion droplets have been used to confine particles for their assembly. When particles are confined at the droplet–solution interface, they could form hollow superstructures called colloidosomes.<sup>9</sup> On the other hand, particles confined inside the droplets can give close-packed globular clusters.<sup>10</sup> In these

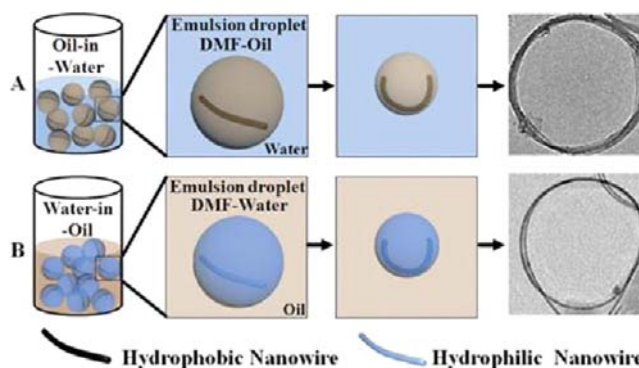


**Figure 1.** Schematics illustrating the coiling of hydrophobic nanofilaments by oil-in-water emulsion (method A) and hydrophilic nanofilaments by water-in-oil emulsion (method B).

examples, the emulsion droplets played mostly a static role, with their surface or body serving as a structural template. An intriguing question following these successes is whether one can exploit the confining effects of droplets to manipulate nanostructures, for example, to induce conformational changes in nanofilaments.

**Received:** October 21, 2012

**Published:** December 17, 2012

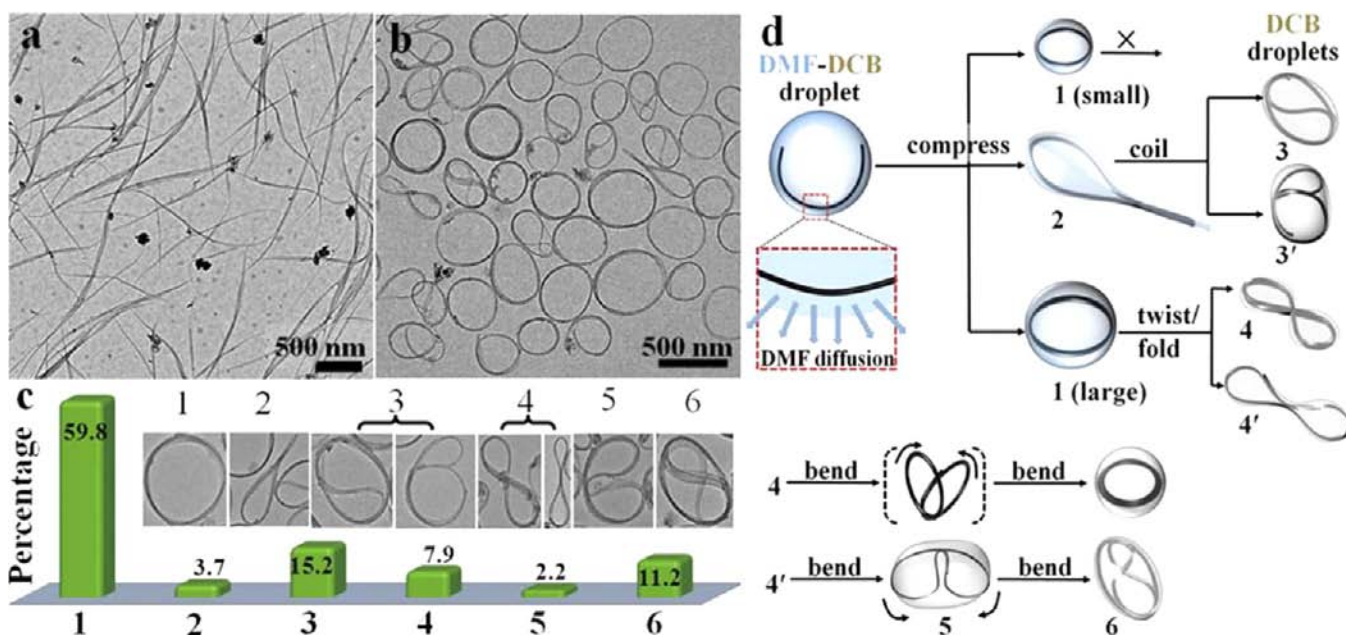


**Figure 2.** TEM images of (a) bundles of single-wall CNTs and (b) CNT rings obtained by method A1. (c) Definition of the ring types and histogram of their percentage in sample b, which was obtained by surveying 403 rings; the examples shown in the insets are not on the same scale. (d) Schematics illustrating the coiling of the various types of CNT rings by method A.

Recently, we discovered that the polymer shells on the surface of Au NWs and CNTs can cause these embedded nanofilaments to coil into rings.<sup>6a,b</sup> Huang and co-workers utilized the rapid evaporation of aerosol droplets to compress the dissolved graphene oxide sheets into crumpled balls.<sup>6c,d</sup> In these systems, the nanostructures were first securely confined by the polymer shells or droplets. Therefore, they were compressed when the droplets transformed in shape or shrunk in volume. There was also a related earlier system using sonication cavities, which upon collapsing could generate shock waves. It has been proposed that such shock waves could exert force to CNT bundles, bending them into rings.<sup>11</sup>

Obviously, the interfaces played a critical role in the shape transformation of these nanostructures:<sup>12</sup> either the polymer–solution interface,<sup>6b</sup> the solution–air interface,<sup>6c,d</sup> or the interface between the fronts of different density in the shock waves.<sup>11</sup> Following these pioneering studies, there are a battery of questions to be answered. How do the interfaces interact with the suspended nanostructures? What are the requirements for these interactions? Can we develop a synthetic methodology based on the general principles?

In this report, we study the general interactions between emulsion droplets and nanofilaments (Figure 1). In light of the new results, we come to the realization that in our previous systems the solvent-swollen polymer shells were merely unified hydrophobic “oil” droplets and that the secure confinement provided by the polymer shells was not even a necessary condition. Thus, the coiling process can simply be induced by oil-in-water emulsions. Without the need of polymer encapsulation, the method is now simpler and more scalable. More importantly, the dynamic formation and shrinking of the emulsion droplets provides a means to give complex high-curvature rings and a “handle” for mechanistic studies. On the other hand, using silica shells as a trapping device, we are able to coil even hydrophilic nanofilaments in reverse water-in-oil emulsions. Given the ready availability and widespread use of emulsions, this work points to the often overlooked mechanical

effects of humble emulsion droplets. It takes only a tiny amount of residue reactants/solvents to form an emulsion, and the resulting effects could be pronounced for fine nanofilaments such as CNTs and ultrathin NWs.

## COILING OF CNTS IN OIL-IN-WATER EMULSION

The well-known “solvent-shifting” method<sup>13</sup> was used to prepare both oil-in-water and water-in-oil emulsions. The general method is to choose a common solvent (e.g., DMF) for water and oil. A small amount of oil is dissolved in DMF and then mixed with a large amount of water. Because DMF is miscible with water but the oil is not, most of the DMF in the oil domain escapes into the water phase. Thus, the “shifting” of the solvent from nonpolar to polar caused the oil to be dispersed in the solution, forming fine droplets.<sup>13a</sup> Similarly, water-in-oil emulsions can also be easily prepared. The main difference in our approaches is that nanofilaments are included in the process and transformed in shape.

Oil-in-water emulsions with enclosed CNTs were formed by the following procedure (Figure 1): Single-wall CNTs of 300 nm to 4  $\mu\text{m}$  in length were dispersed in DMF by high-power tip ultrasonication, giving a transparent dark suspension. As confirmed by transmission electron microscopy (TEM), the CNTs at this step were bundles of about 15–30 nm in width (Figure 2a). High-resolution TEM showed that the individual CNTs in the bundles were parallel to one another, and there was no obvious twisting of the bundles.<sup>14</sup> A small amount of “oil”, namely, 1,2-dichlorobenzene (DCB, 1.2  $\mu\text{L}$ ), was then dissolved in this DMF solution (200  $\mu\text{L}$ ). Upon quick addition of 1 mL of water, the mixture turned turbid, indicating the emulsification of fine DCB droplets. Finally, the CNT product after the above treatment was isolated by centrifugation. As shown in Figure 2b, the product contained mostly ring-like structures with a wide diameter distribution ( $320 \pm 120$  nm).

However, the structural variety of the rings in the product was greater than those prepared previously using polymer shells.<sup>6b</sup> In the sample of Figure 2b, there were known

structures such as simple O-shaped rings (type 1, 59.8%), racket-shaped (type 2, 3.7%), Yin-Yang-shaped (type 3, 15.2%), and 8-shaped (type 4, 7.9%) ring structures. As discussed in our previous papers, 1 was formed by coiling a straight CNT bundle; 2 was formed by bending a bundle followed by parallel packing of its two ends; and 3 was formed by coiling 2 (Figure 2). The formation of 2 may or may not involve oil droplets. However, the formation of 4 must involve at least two stages: Considering the numerous possible conformations of a filament, it is hard to imagine how the complex yet orderly structure of 4 can be directly assembled from a straight filament (otherwise, many random structures should also have been obtained). A large simple ring should form first before it is compressed further to 4, either with or without twisting the ring (4 and 4'). In addition to these known structures, however, there were also B-shaped compressed rings (type 5, 2.2%) and a complex structure that consisted of a twisted 8-shaped ring inside a circular ring (type 6, 11.2%). Close inspection of these structures revealed that they were probably formed by bending and compressing 4 (Figure 2d). That is, a third-stage compression was necessary to achieve the smaller structures of 5 and 6.<sup>14</sup>

The product CNT rings were very stable. They did uncoil after being dispersed in either water, DMF, or DCB, probably because of the strong  $\pi$ - $\pi$  stacking among the CNTs. Even after treating the rings in DMF by high-power tip ultrasonication (1 h), very few straight bundles were found (Figure 3a).<sup>14</sup>

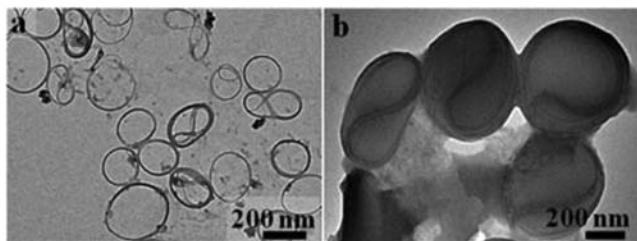


**Figure 3.** TEM images of (a) the resulting CNT rings after treating the as-prepared rings in DMF (method A1) with high-power ultrasonication for 1 h and (b) intermediate droplets trapped by DVB polymerization using method A1.

DCB and DMF were not unique in this process. Other solvent combinations, such as those listed in Table 1, can also

**Table 1.** Oil–Solvent Combinations That Worked for Method A1, After Mixing with a Large Amount of Water<sup>a</sup>

	DMF	N-methylpyrrolidinone	N-vinylpyrrolidinone
1,2-dichlorobenzene	✓	✓	✓
1,4-divinylbenzene	✓	✓	✓
toluene	✓	✓	low yield
cyclohexane	✓	✓	low yield
hexanes	✓	✓	low yield

<sup>a</sup>See the resulting products in the Supporting Information.

be used. A general principle is that the oil must be nonpolar and interact well with the CNTs. In addition, the oil should be first solubilized, and then the oil-carrying solvent should be miscible with water. Such a common solvent can be either DMF, N-methylpyrrolidinone, or N-vinylpyrrolidinone. Thus, upon mixing, emulsion can be generated. Control experiments

showed that the formation of fine droplets was essential: mixing DMF and water without the oil did not give any CNT ring, and it also did not work by using too much oil (vide infra). When 1,4-divinylbenzene (DVB) was used as oil, by in situ polymerization we were able to trap the emulsion droplets with embedded CNT bundles. The resulting products were mostly polymer spheres, with CNT rings located close to the polymer–solvent interface (Figure 3b). This result confirmed that the rings were formed inside the suspended oil droplets before the polymerization.

## MECHANISTIC INVESTIGATIONS

The multistage compression of the CNT rings is counter-intuitive, particularly because the emulsion system only involved water, DMF, and DCB. Should a droplet remain static when interacting with a CNT bundle, there is no obvious mechanism by which the bundle could be compressed more than once. To explain the three-stage compression experienced by 6, we hypothesized that the process may involve continued compression during the rapid shrinking of the droplets, possibly due to the loss of DMF from the oil domains.

To test this hypothesis, we sought to generate emulsion droplets first and then introduce CNT bundles (method A2): 6  $\mu\text{L}$  of DCB was mixed with 1 mL of DMF and then 5 mL of water (the same ratios as method A1) was quickly added to the mixture. The resulting emulsion was incubated for 5 min to allow sufficient time for DMF to leave the DCB domains. A separate DMF solution (200  $\mu\text{L}$ ) containing CNT bundles was first diluted by 600  $\mu\text{L}$  of water (no emulsion was formed in this solution because of the high DMF concentration and absence of DCB). This solution was then added to the above emulsion, and the mixture was incubated for 30 min to allow time for the CNTs to interact with the droplets. In this method, we aim to minimize the complications caused by the rapid mixing of DMF and water. If the loss of DMF from the oil domains is the cause for the complex rings, avoiding it will reduce the formation of such rings. As shown in Figure 4, the resulting product consisted of both rings and straight CNT bundles, but nearly all of the rings were simple O-shaped rings, without 5 and 6. On the basis of the different products, it was clear that the oil droplets behaved differently in methods A1 and A2. The results were indeed consistent with our hypothesis.

Because method A2 provided nearly static droplets, it is a better platform for understanding the basic interactions between droplets and CNT bundles. Demulsification was used to trap intermediates from this process: CNT bundles were allowed to incubate with preformed emulsion for a certain period  $t$ , and then additional DMF (1 to 1 mL of emulsion) was introduced to dissolve away the DCB droplets. The structure of the resulting product was found to be highly dependent on  $t$ . At  $t = 2$  s, no ring was formed, and only straight CNT bundles were recovered (Figure 5a). With increased time, the percentage of rings in the sample increased noticeably.<sup>14</sup> At  $t = 30$  min, about 73% of the bundles formed rings, but further increase of  $t$  did not give more rings. Obviously, it took time to convert the straight CNT bundles. A likely contributing factor is that the bundles must “find” the droplets by diffusion. Such encounter of submicrometer objects requires time, in a way similar to the collision kinetics of particles.<sup>15</sup>

Despite the different yields of these experiments using method A2, there was no apparent difference in the ring shape (i.e., no complex ring). However, when the emulsion was first

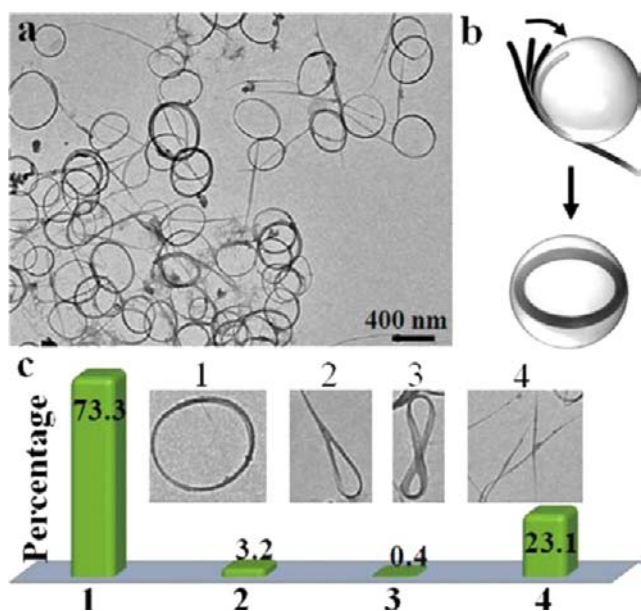


**Figure 4.** (a) TEM image of the CNT rings obtained by method A2 ( $t = 30$  min) and (b) schematics illustrating the coiling process. (c) Histogram of the CNT rings and straight bundles in sample a, which was obtained by surveying 251 bundles/rings.

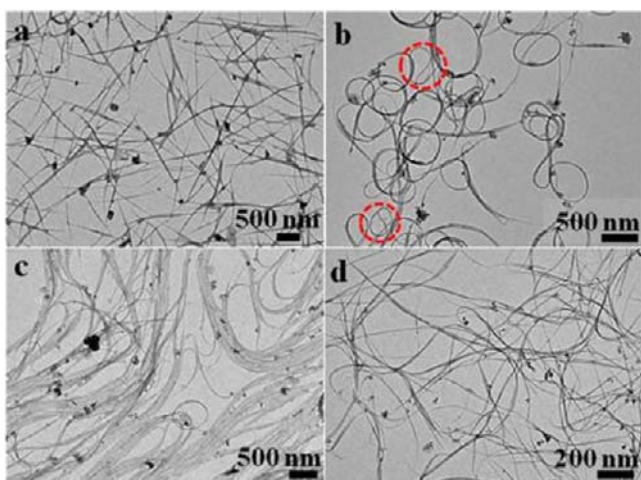


**Figure 5.** TEM images of (a) intermediates trapped by demulsification in method A2 ( $t = 2$  s) and (b) the CNT rings trapped by demulsification in method A1 ( $t = 2$  s), where the complex rings were highlighted by circles. (c, d) Products obtained by using 10 and 0.5  $\mu\text{L}$  of DCB in method A1, respectively.

ripened for 4 h, giving large droplets, addition of CNTs barely gave any ring. Instead, the CNTs aggregated with partial folding (similar to Figure 5c).<sup>14</sup> When the ripened solution was sonicated to break up the large oil droplets before the addition of CNTs, rings were obtained again. Thus, we conclude that the CNT rings were templated by the emulsion droplets. When the droplets are too large, the CNTs cannot establish sufficient overlap to form stable rings. This conclusion was further supported by control experiments: In method A1, when the DCB amount was increased from 1.2 to 10  $\mu\text{L}$  (or an equivalent amount in method A2), very few rings were obtained because the emulsion droplets were too large (Figure 5c). On the other hand, when the amount of DCB was reduced

to 0.5  $\mu\text{L}$ , the average DCB droplets were too small to coil the CNT bundles (Figure 5d).

The fact that hydrophobic CNTs can enter and coil inside preformed static droplets means that the initial confinement by the droplets was not a critical factor. Intuitively, one may think such an initial confinement was necessary for the droplets to exert force to the enclosed CNT bundle. In our earlier works, the polymer shell solidified<sup>16</sup> when DMF was removed from it, and thus the initial confinement was indeed essential.<sup>6a</sup> Even in the presence of DCB,<sup>6b</sup> the polymer domains were probably too viscous for CNTs to enter. However, in the current system without the polymer shells, the new results have demonstrated to us an unexpected possibility. The key issue here is not if the droplet can exert sufficient force to bend the CNT bundle (it obviously can) because the thermal vibration of the bundle driven by random Brownian motion may already be doing it. Rather, the question is if it is favorable for the CNTs to *stay* bent and coiled to fit inside the smaller oil droplets. This is in essence equivalent to the phase transfer of CNTs from water to oil,<sup>17</sup> except that it occurs at the nanoscale with additional strain energy.

A CNT bundle has different solvation energy in water ( $E_{\text{water}}$ ) and in DCB ( $E_{\text{oil}}$ ). The solvation energy can be expressed as eq 2, where  $\gamma$  is the surface tension and  $A$  is the interfacial area.<sup>18</sup> If their difference is larger than the induced strain ( $E_{\text{strain}}$ ), then the bundle would stay bent to enter and remain inside the oil droplet (Figure 4b and eq 1). The strain energy can be expressed as eq 3,<sup>19</sup> where  $Y$  is the Young's modulus of the CNT bundle,  $I$  is area moment of inertia (a factor describing the cross-sectional shape of the filament;  $YI$  describes the flexural rigidity),  $l$  is the length of the CNT bundle, and  $R$  is the radius of the resulting CNT ring. From eq 3, more strain is induced when the CNT bundle is longer or when forming tighter rings. Thus, if the droplet is too small, bending by high curvature becomes unfavorable. Once the first loop is formed, the stacking energy among the loops ( $E_{\text{stacking}}$ ) becomes nonzero, and this term makes the subsequent coiling of additional loops more favorable.

$$\Delta G = E_{\text{oil}} - E_{\text{water}} + (E_{\text{strain}} - E_{\text{stacking}}) < 0 \quad (1)$$

$$E_{\text{solvation}} = \gamma \cdot A \quad (2)$$

$$E_{\text{strain}} = \frac{(YI) \cdot l}{2R^2} \quad (3)$$

The coiling process in method A1 is likely more complicated due to the rapid mixing of DMF and water. Regardless of the specific kinetic pathway, it has to be at least thermodynamically favorable for the CNT bundle to enter and coil inside an oil droplet. Indeed, if the CNTs were rendered hydrophilic by acid treatment,<sup>20</sup> they cannot be coiled into rings using either method A1 or A2.<sup>14</sup>

The kinetic process is relatively straightforward in giving a simple O-shaped ring (Figure 4a). Regardless of where a droplet makes initial contact with a bundle, the bundle should bend near the contact point, so that the nearby CNT sections can maximize their interactions with the oil (or the oil–water interface, depending on the interfacial energies<sup>21</sup>). Continued bending near the new contact points will lead to a circular loop. This first loop can serve as a template for the subsequent coiling and stacking of multiple loops.

However, once a ring is formed, it is not easy to explain its bending and twisting to form more complex structures such as

6. Considering its smooth curvatures, there is no reason for the bundle (unless it is broken) to bend sharper than the local curvature of the oil droplet, which induces additional strain without extra driving force. Moreover, given the few ingredients in the system, there is no obvious candidate for a different type of driving force. In our earlier work, the origin of the double-stage compression experienced by the eight-shaped CNT rings was not understood.<sup>6b</sup> Given the multiple components in that system, we can at least propose that the compression was caused by the sequential loss of DMF and DCB from the polymer domains, but in the current simpler system, this hypothesis cannot explain the triple-stage compression experienced by 6.

If the size of the droplet was continually decreasing during the process, then the CNT ring could be folded again to fit inside the reduced oil domain under the same driving force. If so, the process must have occurred very rapidly at the initial stage of mixing and during the diffusion of DMF from the oil domains. The structural vibration of the CNT bundle (part of its random thermal motion) may assist its coiling. However, since the coiling process is well behaved in both methods (not giving completely random structures), the random vibration is important but probably not the dominant factor.

In method A1, we also used demulsification to trap intermediates ( $t = 2$  s). As shown in Figure 5b, a large amount of CNT rings were obtained (70%), and multiply compressed structures can be observed. Hence, most of the rings were formed almost immediately after the mixing, in clear contrast to method A2. If the droplets in method A1 were fully formed before encountering CNTs, the results should have been identical in terms of ring structure. Moreover, if the CNTs and DCB droplets were formed separately in the solution, their encounter would have required a time scale similar to that of method A2. Therefore, the DCB droplets probably formed together with CNTs during the initial stage of “solvent-shifting” ( $t \leq 2$  s), when the droplets were most probably not static. This result thus supported our hypothesis on the multiple compressions.

Upon addition of water to the DMF solution, their violent mixing separates the DMF domains into small pockets, where DMF can be continuously removed via the interface with water. Thus, both DCB and CNTs could be trapped inside such solution pockets, giving oil droplets. When a droplet reaches a critical size, the trapped CNT bundle is forced to coil into a ring. Continued loss of DMF further decreases the droplet size, but once a CNT ring is formed, it cannot be coiled tighter because of the friction among the loops. As a result, the ring is forced to squash and bend to fit inside the reduced volume. This process can continue until the total removal of DMF or when the induced strain exceeds the driving force. From this perspective, the final structure of a complex ring is determined by the initial content of the DCB/DMF in the droplet and the size of the CNT ring, both of which should have wide distributions.

In light of these new mechanistic understandings, we tried to re-examine the role of polymer shells in our previous systems. The main difference of this work is that the CNT-containing droplets were only made of DMF and DCB, whereas in previous works the “droplets” were made of (a) polymer, DMF, and residue amount of oleylamine<sup>6a</sup> or (b) polymer, DMF, and DCB.<sup>6b</sup> Previously, we assigned the dominant role to the polymer shells, whereas DMF and DCB were merely swelling the polymer domains improving their mobility. In light of the

new results, we tried to understand the separate roles played by the different ingredients. However, as far as mechanical effects are concerned, the ring formation from nanofilaments was very similar with and without the polymer shells. In Table 1, toluene was a mimic for the polystyrene shell, and the same coiling effects were observed. From this perspective, the polymer “droplets” were not particularly different. It appeared that the mixture of polymer, DMF, and oil was essentially a unified droplet; it would be meaningless to distinguish their individual roles. The only different role of the polymer shells was in the formation of oil droplets: they served as liquid pockets that helped in concentrating oleylamine or DCB in these domains. Thus, much less oil was required than that used in our current experiments.

## ■ SCALABLE SYNTHESIS OF CNT RINGS

In this new synthetic system using only emulsion droplets, a clear advantage is that the process is significantly simpler and more scalable. Without the need of polymer shells, all one has to do is to mix a few solutions and filtrate: 300 mL of water was stirred violently, and 60 mL of CNTs dispersed in DCB/DMF (the same ratios as above) was added slowly. After 10 min, 30 mL of DMF was added to cause demulsification, and the mixture was filtrated to collect the CNT rings (Figure 6). The

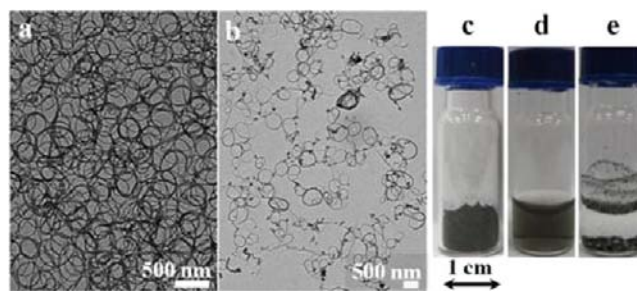


**Figure 6.** Scale-up syntheses of CNT rings by method A1, showing samples prepared from (a) high-quality and (b, c) cheap CNTs and photographs of (d) sample c dispersed in water by ultrasonication and (e) straight as-purchased CNTs dispersed in water.

powder form of the resulting CNT rings in Figure 6c can be readily dispersed in water by gentle sonication (Figure 6d). In contrast, straight CNTs are very difficult to disperse (Figure 6e). This was true in other solvents: the CNT rings were in general more easily dispersed, and the resulting colloids were more stable.<sup>14</sup> The main reason is that the rings cannot pack well with each other because of their different diameters, whereas the straight CNTs can strongly stack with each other in parallel.

## ■ COILING NANOFILAMENTS USING WATER-IN-OIL EMULSIONS

As discussed, the fundamental interactions between droplets and nanofilaments should be more general than the oil-in-water emulsion. Thus, the next challenge is to design experiments in water-in-oil emulsion systems. For the nanofilaments to like water droplets, hydrophilic ones have to be used. Moreover, they have to be thin enough to bend easily. We need to create situations where the nanofilaments are driven from the bulk oil phase into tiny water droplets, overcoming the cost of induced strain. After many trials, we realized that the main difficulty in this system is that the interactions among the hydrophilic

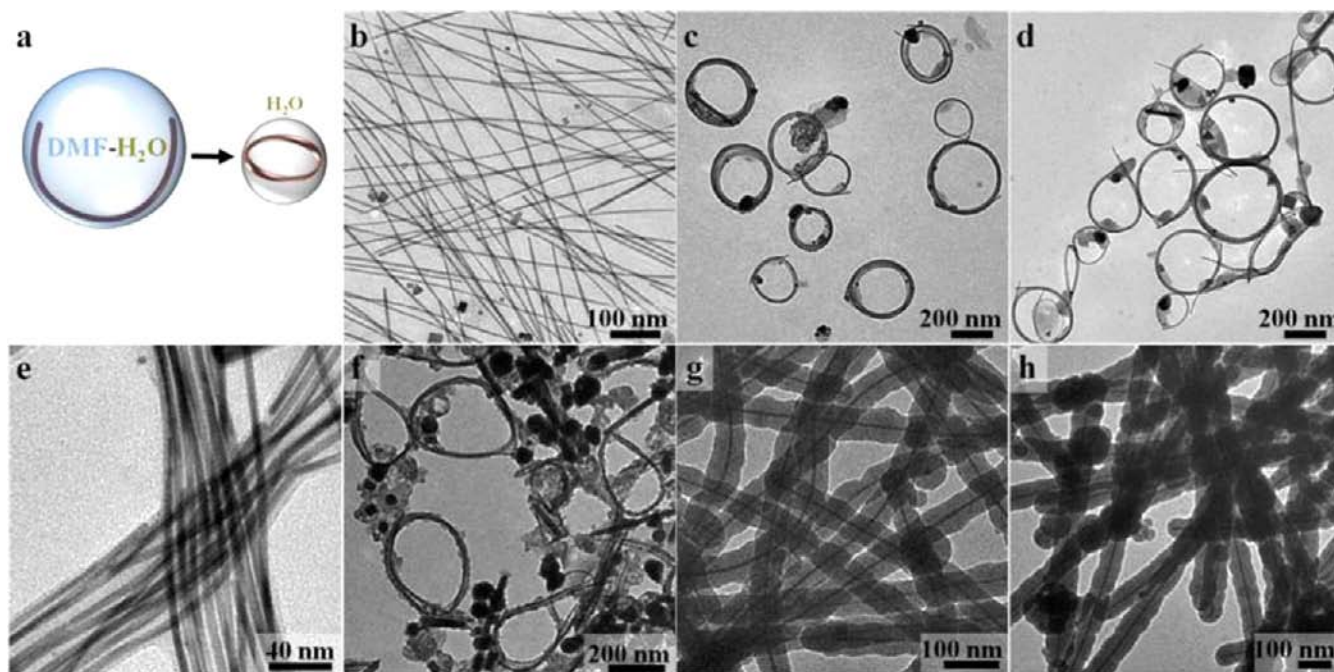


**Figure 7.** (a) Schematics illustrating the coiling process of hydrophilic Pd NWs in water-in-oil emulsion (method B) and TEM images of (b) as-prepared Pd NWs; (c) silica-coated Pd NW rings obtained using water-in-DCB emulsion; (d) silica-coated Pd NW rings obtained using water-in-toluene emulsion; (e) Pd NWs coated with a thin silica shell; (f) after coiling sample (e) using water-in-DCB emulsion; (g) Pd NWs coated with a thick silica shell; (h) after treating sample (g) using water-in-DCB emulsion.

nanofilaments were not strong enough to hold the rings in place. Even after they were coiled into rings, they could easily uncoil when they were no longer confined by the water droplets. In the following, we adapted a silica-encapsulation method for use inside the emulsion droplets, so that the coiled nanostructures could be trapped.

We choose thin Pd NWs<sup>22,23</sup> for the case study. The NWs were synthesized following the literature procedures.<sup>23</sup> They were typically 10 nm in diameter and about 3  $\mu\text{m}$  in length (Figure 7b). Coated with poly(vinylpyrrolidone) (PVP), they can be readily dispersed in water. They were included in reverse water-in-oil emulsion by the “solvent-shifting” method: As-synthesized Pd NWs were concentrated by centrifugation and then dispersed in DMF (40  $\mu\text{L}$ ) and aqueous  $\text{NH}_3\cdot\text{H}_2\text{O}$  (25%, 3  $\mu\text{L}$ ). A large amount of oil (DCB or toluene, 1 mL) was then quickly added to this solution, and the mixture turned turbid immediately, indicating emulsification of water droplets. A small amount of tetraethyl orthosilicate (TEOS, 3  $\mu\text{L}$ ) was then added. They were intended to be transferred into the water droplets and catalyzed by the  $\text{NH}_3\cdot\text{H}_2\text{O}$  therein.

As shown in Figure 7c,d, most of the Pd NWs were compressed into rings, and silica shells formed on their surface. Control experiments without using TEOS and  $\text{NH}_3\cdot\text{H}_2\text{O}$  gave hardly any rings, indicating the critical role of silica shells in retaining the ring structures. The rings were about 200–400 nm in diameter. Similar to the above system, the relative volume of the aqueous phase was a critical factor. Too much or too little water (<1  $\mu\text{L}$  or >10  $\mu\text{L}$ ) led to unsuccessful coiling of the NWs. When DCB was used as the oil giving water-in-DCB emulsion, the ends of the Pd NWs stacked well along the resulting rings, and thus, they cannot be easily distinguished. However, when water-in-toluene emulsion was used, the ends often stuck out from the rings. On the basis of the number of such ends, it can be learned that most of the compact rings were made of a single Pd NW (Figure 7d), but there were also

quite a few loose rings made of multiple NWs.<sup>14</sup> In contrast to the CNT rings prepared from oil-in-water emulsion, there were very few complex Pd rings with high curvature (types 3–6 in Figure 2). Mostly likely, it was because the 10 nm Pd NWs were stiffer than the CNT bundles.

As a means to modulate the stiffness of the Pd NWs, we coat them with silica shells before treating them with emulsion. When the initial silica shells were thin ( $\sim 2$  nm, Figure 7e), rings could still be found in the coiled products (Figure 7f). However, when the initial silica shells were increased to 18 nm, the Pd NWs could no longer be coiled (Figure 7g,h).

A second example we chose was hydrophilic  $\text{MnO}_2$  NWs that were about 15 nm in diameter and 2–5  $\mu\text{m}$  in length (Figure 8a). They were prepared in the water–octanol system<sup>24</sup> and appeared to be thin enough to bend. The as-synthesized  $\text{MnO}_2$  NWs were purified by centrifugation and redispersed into a solution of PVP in DMF. The mixture was then incubated at 70  $^\circ\text{C}$  for 2 h. Using the same experimental conditions as those used above for Pd NWs, the  $\text{MnO}_2$  NWs were coiled into rings by applying silica encapsulation during the formation of water-in-toluene emulsion (Figure 8b). The diameter of the  $\text{MnO}_2$  rings was larger than those of the Pd and CNT rings, probably because the 15 nm  $\text{MnO}_2$  NWs were much stiffer.

Hydrophilic CNTs were prepared for use in water-in-oil emulsion, to compare with the CNT rings in the oil-in-water emulsion. As-purchased CNTs (NanoIntegris) were treated by concentrated  $\text{HNO}_3$  and then purified (Figure 8c). Such oxidized CNTs were readily dispersed into a mixture of DMF (40  $\mu\text{L}$ ) and water (2  $\mu\text{L}$ ); a large amount of oil (DCB or toluene, 1 mL) was then added. In the resulting products, many loose rings can be found (Figure 8d). In this system, silica encapsulation was not necessary to retain the rings. Probably, the entangling or the local stacking interactions among the oxidized CNTs were strong enough to hold the rings in place.

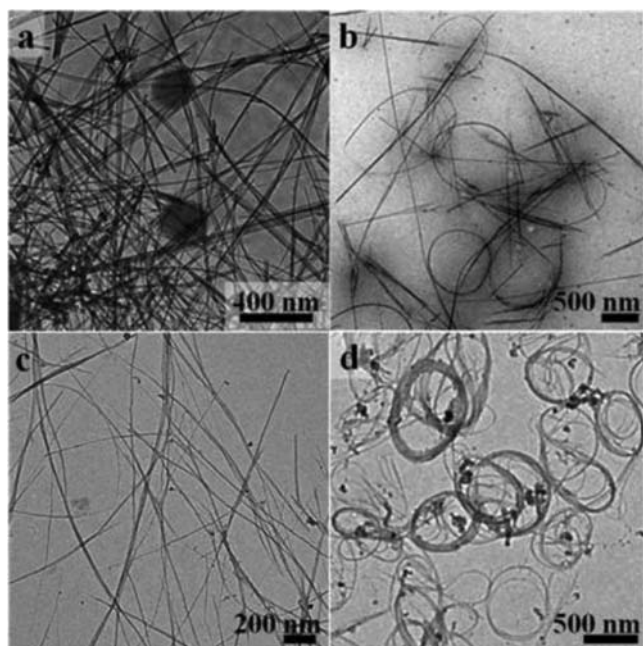


**Figure 8.** TEM images of (a) as-prepared MnO<sub>2</sub> NWs, (b) silica-coated MnO<sub>2</sub> NW rings obtained by method B in water-in-toluene emulsion, (c) hydrophilic CNTs, and (d) CNT rings by coiling sample c in water-in-DCB emulsion.

However, the oxidized CNTs appeared to be unable to pack closely like those in Figure 2b.

## OVERVIEW OF THE MECHANISMS

For clarity, we will separate the arguments of thermodynamics and kinetics. Only the energies involved in the phase transfer and conformational changes of the nanofilaments are considered; energies involved in chemical reactions, defects, etc. are excluded.

Let us first consider the thermodynamics of the method A2: When a straight CNT bundle encounters an emulsion droplet, the bundle “wants” to transfer from the aqueous phase to the oil phase. The starting state is a straight CNT bundle in water, whereas the final state is a coiled ring inside the oil droplet. Thus, the coiling process is driven by the difference of the solvation energy at the two states ( $E_{\text{oil}} - E_{\text{water}}$ ). When this difference is larger than the induced strain energy, the hydrophobic CNTs would bend to minimize their exposed segments in water. Once the second loop forms, the stacking energy among the loops provides an additional driving force. This mechanism is consistent with the experiments: When CNTs are modified to become hydrophilic (more negative  $E_{\text{water}}$  means less driving force in eq 1), they cannot be coiled using oil-in-water emulsion. The size of the oil droplet is also of importance: With very small oil droplets, the induced strain is too much (larger  $E_{\text{strain}}$  gives less negative  $\Delta G$ ), making the coiling process unfavorable; with very large oil droplets, the bundles can simply dissolve in them without coiling (more favorable because  $E_{\text{strain}} = 0$ ).

In method A1, the DCB/DMF droplets decrease in size as DMF escapes into the water phase. Let us only consider the very instant when the bending of CNTs or the compression of rings occur. Thus, the DMF content in the oil droplet can be treated as constant during that particular instant. At a certain point during solvent shifting, the oil domain becomes too small

for the entrapped CNT bundle. If a bundle or ring does not deform, part of it has to reach out into the water phase. Thus, the bending/compressing process can still be analyzed using eq 1, except that the  $E_{\text{oil}}$  is now the solvation energy of the CNT bundle in the DCB/DMF mixture. As DMF escapes, the oil domain becomes less polar, and the  $E_{\text{oil}}$  becomes more negative, providing more driving forces in eq 1. Given the fact that complex rings are formed, the difference in solvation energies is obviously large enough to overcome the maximum induced strains when repeatedly compressing a ring.

Having a sufficient thermodynamic driving force only means that the process can potentially occur. Roughly speaking, there are two possible scenarios: (1) A CNT bundle may repeatedly coil and uncoil, until it finds a most stable structure (i.e., thermodynamically controlled process). (2) A CNT bundle may be coiled only once (kinetically controlled): As soon as a ring is formed, the strong stacking among the loops makes it impossible to uncoil and try a different conformation. Moreover, the ring cannot be tightened to a smaller diameter because the “friction” among the CNTs prevents sliding. From our results, the product CNT rings do not uncoil in either water, DMF, or DCB, indicating that the stacking energy therein is larger than the strain energy. For the complex rings formed by method A2, should they be able to uncoil and then coil again into a ring of similar diameter, the resulting ring should have less strain and more stacking, both of which make the  $\Delta G$  more negative in eq 1. Therefore, the fact that the high-energy complex rings are obtained in experiments suggests that scenario (1) is incorrect. Thus, how exactly a ring is coiled depends on the kinetic pathways, as is detailed in the following.

In method A2, while the CNT bundles are unstable in water, they cannot be coiled unless they can find the oil droplets by random “collision”. This process takes time, allowing us to trap different coiling intermediates by demulsification (Figure 5a). Once a CNT bundle encounters an oil droplet, it is forced to coil, most probably by curving around the oil droplet (Figure 4). Given the small size of a CNT bundle, its Brownian motion driven by the random collision with solvent molecules is likely very significant. Thus, we think that the bundle is highly dynamic; it should be constantly moving, rotating, and vibrating. As such, analysis of the static forces between the oil droplet and the CNT bundle is inappropriate. As long as there is sufficient driving force, a bundle should coil and enter an oil droplet, and the process is likely assisted by its structural vibration. After forming a ring, because the size of the oil droplets is not changing, there is no obvious pathway by which the ring can be compressed further to a more strained structure of smaller size. Therefore, obtaining the simple rings in Figure 4a is consistent with the mechanism.

In contrast, in method A1 the size of the oil domains changes during the solvent shifting, allowing pathways that lead to the high energy complex rings. Given the numerous possible conformations of a filament, a direct path leading to an orderly structure at a high energy state is inconceivable. Thus, we believe that the CNT bundles are compressed multiple times. This process occurs in the short period of solvent shifting (<2 s), as confirmed by our demulsification results (Figure 5b). As a large amount of water is added to a DCB/DMF mixture, the oil domain is instantaneously dispersed into small pockets, entrapping the dissolved CNTs. As DMF escapes from the oil domain and the droplet size reaches a critical size, the entrapped CNT bundle is forced to coil into a ring. As far as this single-step compression is concerned, a simple ring is

favored because it is the lowest energy structure within the confined volume. Then, as the oil domain shrinks further, the ring becomes too large to fit inside, causing it to be folded again to give a complex ring. As discussed above, we think the structural vibration of the CNT bundles and rings is highly dynamic. It is thus conceivable that the determining factor is the random configuration of a ring at the very instant of compression. This argument explains the formation of twisted and nontwisted rings (4 and 4'). It should be noted that there are also many possible conformations in folding a ring. Among them, the type 4 and 4' rings are probably the lower energy ones during the second-step compression. Similarly, the triply compressed type 6 rings can also be explained: As long as the oil domain is small enough and the induced strain is not too large, the CNT ring "wants" to be folded again to remain in the oil domain. In each of the above three steps, a relatively low energy structure is obtained, and yet the final complex ring is at a high energy state. This is because the environment is changing, namely, the size of the oil domain and the DCB/DMF content therein. At the final step of compression, the ring trapped inside a small volume simply cannot go back to the old environment (a large droplet) and use the lower energy pathways to make a small ring.

For coiling nanofilaments by water-in-oil emulsion, the fact that coiling can occur suggests that the underlying mechanism should be similar. However, the Pd and MnO<sub>2</sub> NWs are too stiff to give complex rings, and their stacking is not as good as that among the CNTs. Thus, the use of silica coating is necessary, causing complications. These limitations make it difficult to gain further mechanistic insights in this system.

## CONCLUSION

In summary, we exploited a very simple and old system, emulsion, for the generic fabrication of nanoscale rings from both hydrophobic and hydrophilic nanofilaments. In our daily life, macroscopic rings are useful structural components, but in self-assembly, they are up until now very difficult to make. Emulsions can be readily prepared, offering a large number of tiny droplets for interacting with nanostructures. Hence, our work provides a new synthetic methodology for nanoscale rings and a basis for rational exploitation of emulsion systems.

Emulsions are of common occurrence in chemical synthesis, when two immiscible liquids or reactants are mixed. In particular, sonication can easily break up large droplets and enhance the vibration of nanostructures, facilitating their interactions. By studying the effects on nanofilaments, this work also provides a rare means to probe the complex interactions between nanostructures and emulsion droplets. The understanding of the mechanical effects of such droplets is of importance for interpreting their often unsuspected roles when they coexist with nanowires or nanosheets.

## EXPERIMENTAL SECTION

**Materials and Characterization Methods.** All chemical reagents were used as purchased without further purification. High-quality, single-wall carbon nanotubes (CNTs) (carbonaceous purity 99%) with length of 300 nm to 4  $\mu$ m were purchased from NanoIntegris; single-wall CNTs (carbonaceous purity 90%, metal content 4–8% in weight) were purchased from Carbon Solution, Inc. All other chemicals were purchased from Sigma Aldrich. Deionized water (resistance >18.2 M $\Omega$ /cm) was used in all reactions. Copper specimen grids (300 mesh) with carbon film (referred to as TEM grids in the text) were purchased from Beijing XXBR Technology Co.

Transmission electron microscopy (TEM) images were collected on a JEM-1400 (JEOL) operated at 100 kV. High-resolution TEM images were obtained by using a JEOL JEM-2100F TEM with an accelerating voltage of 200 kV.

**Synthesis of CNT Rings Using Oil-in-Water Emulsion. Method A1.** In a typical procedure, single-wall CNTs (NanoIntegris) were dispersed in DMF with a tip sonicator (130 W ultrasonic processor, Sonics & Materials, Inc.) until a transparent black suspension was obtained. The concentration of the formed suspension was as high as  $\sim$ 0.1 mg/mL, and then 1.2  $\mu$ L of 1,2-dichlorobenzene (DCB) was added into the suspension (200  $\mu$ L) and vortexed to give a homogeneous mixture. Subsequently, 1 mL of water was introduced to the mixture in one shot, and the mixture was changed from transparent into turbid immediately, indicating emulsification. Finally, the emulsion was kept for 10 min at room temperature, and the product was isolated by centrifugation at 16 000g for 30 min and characterized by TEM.

**Method A2.** In a typical procedure, 6 mL of water was added into the mixture of DMF (1 mL) and DCB (6  $\mu$ L). The resulting inducing emulsion was incubated for 5 min to allow sufficient time for DMF to leave the oil domains. Subsequently, 200  $\mu$ L of CNT suspension in DMF was diluted by water (600  $\mu$ L) and then added into the above emulsions, and the mixture was vortexed. The mixture was kept for 30 min at room temperature, and the product was isolated by centrifugation at 16 000g for 30 min.

**Scaled-Up Synthesis of CNT Rings.** In a typical procedure,  $\sim$ 5.0 mg of CNTs (Carbon Solution, Inc.) was dispersed into the mixture of DMF (60 mL) and DCB (360  $\mu$ L) by a tip sonicator. An amount of 300 mL of water was stirred vigorously, and the CNT suspension was added slowly. The mixture was kept at room temperature for 10 min, and then  $\sim$ 30 mL of DMF was added to demulsify the solution. The products were collected by vacuum filtration (nylon membrane filters, 47 mm in diameter, 0.2  $\mu$ m pore size).

**Synthesis of Pd Rings Using Water-in-Oil Emulsion. Synthesis of Pd Nanowires.** Pd NWs were synthesized according to the literature with some modification.<sup>23</sup> In a typical procedure, 17.7 mg of PdCl<sub>2</sub>, 300 mg of NaI, and 800 mg of PVP ( $M_w = 40\ 000$ ) were added into deionized water (12 mL), and the mixture was stirred for 10 min at room temperature. The resulting dark red solution was transferred into a 25 mL Teflon-lined autoclave and then heated at 200  $^{\circ}$ C for 2 h in a digital oven before cooling to room temperature. The final black product was isolated by centrifugation at 16 000g for 20 min and dispersed into DMF (12 mL).

**Synthesis of Pd Rings by Method B.** Aqueous NH<sub>3</sub>·H<sub>2</sub>O (25%, 3  $\mu$ L) was added into Pd NW solution in DMF (40  $\mu$ L) and vortexed. Afterward, 1 mL of DCB (or toluene) was added in one shot, followed by 3  $\mu$ L of tetraethyl orthosilicate (TEOS). The transparent solution turned opaque immediately. The mixture was heated at 60  $^{\circ}$ C for 30 min to facilitate silica formation. The final product was separated by centrifugation at 7000g for 10 min.

Similarly, Pd NWs precoated with a silica shell using the Stöber method<sup>25</sup> were also studied in method B.

**Synthesis of  $\alpha$ -MnO<sub>2</sub> Rings in Water-in-Oil Emulsion.**  $\alpha$ -MnO<sub>2</sub> NWs were prepared using a previously reported method with some modifications.<sup>24</sup> Briefly, 0.49 g of Mn(CH<sub>3</sub>COO)<sub>2</sub>·4H<sub>2</sub>O, 0.46 g of (NH<sub>4</sub>)<sub>2</sub>S<sub>2</sub>O<sub>8</sub>, and 0.13 g of (NH<sub>4</sub>)<sub>2</sub>SO<sub>4</sub> were dissolved into 10 mL of deionized water, and then 30 mL of 1-octanol were added. The resulting solution was transferred into a 45 mL Teflon-lined autoclave and heated at 140  $^{\circ}$ C for 12 h in a digital oven. The as-prepared product was collected by centrifugation and washed with deionized water and absolute ethanol. Finally, the  $\alpha$ -MnO<sub>2</sub> NWs were dispersed into 10 mL of PVP solution in DMF (1%) and incubated at 70  $^{\circ}$ C for 2 h.

The modified  $\alpha$ -MnO<sub>2</sub> NWs (40  $\mu$ L, in DMF) were mixed with 3  $\mu$ L of aqueous NH<sub>3</sub>·H<sub>2</sub>O (25%) by vortex. Then, 1 mL of toluene was added in one shot, followed by 3  $\mu$ L of TEOS. The resulting mixture was heated at 40  $^{\circ}$ C for 30 min. The product obtained was collected by centrifugation at 4500g for 15 min.

**Synthesis of Hydrophilic CNT Rings in Water-in-Oil Reverse Emulsion.** Hydrophobic CNTs were obtained by a reported

method.<sup>20</sup> Briefly, CNTs (NanoIntegris) were refluxed in concentrated nitric acid (69%) for 12 h. The oxidized CNTs obtained were washed with deionized water via three cycles of centrifugation and then redispersed in DMF to form ~0.1 mg/mL suspension.

Deionized water (2  $\mu$ L) was added into 40  $\mu$ L of the oxidized CNT suspension in DMF and vortexed. An amount of 1 mL of DCB (or toluene) was added in one shot, and the turbid mixture obtained was centrifuged at 16 000g for 30 min.

## ■ ASSOCIATED CONTENT

### ● Supporting Information

Details of experimental procedures, TEM images, and schematics illustrating the volume change of the droplets. This material is available free of charge via the Internet at <http://pubs.acs.org>.

## ■ AUTHOR INFORMATION

### Corresponding Author

hongyuchen@ntu.edu.sg

### Notes

The authors declare no competing financial interest.

## ■ ACKNOWLEDGMENTS

The authors thank the financial support from the A\*Star (SERC 102-150-0053) and NRF (CRP-4-2008-06) of Singapore.

## ■ REFERENCES

- (1) (a) Xia, Y. N.; Yang, P. D.; Sun, Y. G.; Wu, Y. Y.; Mayers, B.; Gates, B.; Yin, Y. D.; Kim, F.; Yan, Y. Q. *Adv. Mater.* **2003**, *15*, 353. (b) Buck, M. R.; Bondi, J. F.; Schaak, R. E. *Nat. Chem.* **2012**, *4*, 37. (c) Wang, Y.; Chen, G.; Yang, M. X.; Silber, G.; Xing, S. X.; Tan, L. H.; Wang, F.; Feng, Y. H.; Liu, X. G.; Li, S. Z.; Chen, H. Y. *Nat. Commun.* **2010**, *1*, 87. (d) Wang, F.; Han, Y.; Lim, C. S.; Lu, Y. H.; Wang, J.; Xu, J.; Chen, H. Y.; Zhang, C.; Hong, M. H.; Liu, X. G. *Nature* **2010**, *463*, 1061. (e) Wang, Y.; Xu, J.; Wang, Y. W.; Chen, H. Y. *Chem. Soc. Rev.* **2012**, DOI: 10.1039/C2CS35332F. (f) He, W. W.; Wu, X. C.; Liu, J. B.; Zhang, K.; Chu, W. G.; Feng, L. L.; Hu, X. N.; Zhou, W. Y.; Xie, S. S. *Langmuir* **2010**, *26*, 4443.
- (2) (a) Ghosh, A.; Fischer, P. *Nano Lett.* **2009**, *9*, 2243. (b) Paxton, W. F.; Kistler, K. C.; Olmeda, C. C.; Sen, A.; Angelo, S. K.; St; Cao, Y. Y.; Mallouk, T. E.; Lammert, P. E.; Crespi, V. H. *J. Am. Chem. Soc.* **2004**, *126*, 13424. (c) Qin, L. D.; Banholzer, M. J.; Xu, X. Y.; Huang, L.; Mirkin, C. A. *J. Am. Chem. Soc.* **2007**, *129*, 14870. (d) Yang, Z. B.; Sun, X. M.; Chen, X. L.; Yong, Z. Z.; Xu, G.; He, R. X.; An, Z. H.; Li, Q. W.; Peng, H. S. *J. Mater. Chem.* **2011**, *21*, 13772.
- (3) Gao, W.; Sattayasamitsathit, S.; Manesh, K. M.; Weihs, D.; Wang, J. *J. Am. Chem. Soc.* **2010**, *132*, 14403.
- (4) (a) Wang, Y.; Wang, Q. X.; Sun, H.; Zhang, W. Q.; Chen, G.; Wang, Y. W.; Shen, X. S.; Han, Y.; Lu, X. M.; Chen, H. Y. *J. Am. Chem. Soc.* **2011**, *133*, 20060. (b) Feng, Y. H.; He, J. T.; Wang, H.; Tay, Y. Y.; Sun, H.; Zhu, L. F.; Chen, H. Y. *J. Am. Chem. Soc.* **2012**, *134*, 2004.
- (5) (a) Zheng, M.; Ke, C. H. *Small* **2010**, *6*, 1647. (b) Yin, A. X.; Min, X. Q.; Zhang, Y. W.; Yan, C. H. *J. Am. Chem. Soc.* **2011**, *133*, 3816. (c) Cong, H. P.; Ren, X. C.; Wang, P.; Yu, S. H. *ACS Nano* **2012**, *6*, 2693. (d) Huang, X. Q.; Tang, S. H.; Yang, J.; Tan, Y. M.; Zheng, N. F. *J. Am. Chem. Soc.* **2011**, *133*, 15946. (e) Zhao, M. Q.; Zhang, Q.; Tian, G. L.; Huang, J. Q.; Wei, F. *ACS Nano* **2012**, *6*, 4520. (f) Zhang, Q.; Zhao, M. Q.; Tang, D. M.; Li, F.; Huang, J. Q.; Liu, B. L.; Zhu, W. C.; Zhang, Y. H.; Wei, F. *Angew. Chem., Int. Ed.* **2010**, *49*, 3642. (g) Cohen, A. E.; Mahadevan, L. *Proc. Natl. Acad. Sci. U.S.A.* **2003**, *100*, 12141. (h) Sano, M.; Kamino, A.; Okamura, J.; Shinkai, S. *Science* **2001**, *293*, 1299. (i) Zu, M.; Lu, W. B.; Li, Q. W.; Zhu, Y. T.; Wang, G. J.; Chou, T. W. *ACS Nano* **2012**, *6*, 4288. (j) Zhu, L. F.; Shen, X. S.; Zeng, Z. Y.; Wang, H.; Zhang, H.; Chen, H. Y. *ACS Nano* **2012**, *6*, 6033. (k) Ji, X. Y.; Zhao, M. Q.; Wei, F.; Feng, X. Q. *Appl. Phys. Lett.* **2012**, *100*, 263104.
- (6) (a) Xu, J.; Wang, H.; Liu, C. C.; Yang, Y. M.; Chen, T.; Wang, Y. W.; Wang, F.; Liu, X. G.; Xing, B. G.; Chen, H. Y. *J. Am. Chem. Soc.* **2010**, *132*, 11920. (b) Chen, L. Y.; Wang, H.; Xu, J.; Shen, X. S.; Yao, L.; Zhu, L. F.; Zeng, Z. Y.; Zhang, H.; Chen, H. Y. *J. Am. Chem. Soc.* **2011**, *133*, 9654. (c) Luo, J. Y.; Jang, H. D.; Sun, T.; Xiao, L.; He, Z.; Katsoulidis, A. P.; Kanatzidis, M. G.; Gibson, J. M.; Huang, J. X. *ACS Nano* **2011**, *5*, 8943. (d) Chen, Y. T.; Guo, F.; Jachak, A.; Kim, S. P.; Datta, D.; Liu, J. Y.; Kulaots, I.; Vaslet, C.; Jang, H. D.; Huang, J. X.; Kane, A.; Shenoy, V. B.; Hurt, R. H. *Nano Lett.* **2012**, *12*, 1996.
- (7) Gao, P. X.; Mai, W. J.; Wang, Z. L. *Nano Lett.* **2006**, *6*, 2536.
- (8) Ismagilov, R. F.; Schwartz, A.; Bowden, N.; Whitesides, G. M. *Angew. Chem., Int. Ed.* **2002**, *41*, 652.
- (9) (a) Dinsmore, A. D.; Hsu, M. F.; Nikolaidis, M. G.; Marquez, M.; Bausch, A. R.; Weitz, D. A. *Science* **2002**, *298*, 1006. (b) Noble, P. F.; Cayre, O. J.; Alargova, R. G.; Velev, O. D.; Paunov, V. N. *J. Am. Chem. Soc.* **2004**, *126*, 8092. (c) Pan, Y.; Gao, J. H.; Zhang, B.; Zhang, X. X.; Xu, B. *Langmuir* **2010**, *26*, 4184. (d) Jiang, S.; Schultz, M. J.; Chen, Q.; Moore, J. S.; Granick, S. *Langmuir* **2008**, *24*, 10073. (e) Zhang, L. F.; Granick, S. *Nano Lett.* **2006**, *6*, 694.
- (10) (a) Manoharan, V. N.; Elssesser, M. T.; Pine, D. J. *Science* **2003**, *301*, 483. (b) Cho, Y. S.; Yi, G. R.; Lim, J. M.; Kim, S. H.; Manoharan, V. N.; Pine, D. J.; Yang, S. M. *J. Am. Chem. Soc.* **2005**, *127*, 15968. (c) Sacanna, S.; Kegel, W. K.; Philipse, A. P. *Phys. Rev. Lett.* **2007**, *98*, 158301. (d) Velev, O. D.; Lenhoff, A. M.; Kaler, E. W. *Science* **2000**, *287*, 2240. (e) Kim, S. H.; Cho, Y. S.; Jeon, S. J.; Eun, T. H.; Yi, G. R.; Yang, S. M. *Adv. Mater.* **2008**, *20*, 3268.
- (11) Martel, R.; Shea, H. R.; Avouris, P. *Nature* **1999**, *398*, 299.
- (12) Chen, Q.; Bae, S. C.; Granick, S. *Nature* **2011**, *469*, 381.
- (13) (a) Horn, D.; Rieger, J. *Angew. Chem., Int. Ed.* **2001**, *40*, 4331. (b) Aubry, J.; Ganachaud, F.; Addad, J. P. C.; Cabane, B. *Langmuir* **2009**, *25*, 1970.
- (14) See Supporting Information for details.
- (15) Wang, X. J.; Li, G. P.; Chen, T.; Yang, M. X.; Zhang, Z.; Wu, T.; Chen, H. Y. *Nano Lett.* **2008**, *8*, 2643.
- (16) (a) Tan, L. H.; Xing, S. X.; Chen, T.; Chen, G.; Huang, X.; Zhang, H.; Chen, H. Y. *ACS Nano* **2009**, *3*, 3469. (b) Liu, C. C.; Chen, G.; Sun, H.; Xu, J.; Feng, Y. H.; Zhang, Z.; Wu, T.; Chen, H. Y. *Small* **2011**, *7*, 2721.
- (17) Wang, R. K.; Park, H. O.; Chen, W. C.; Silvera-Batista, C.; Reeves, R. D.; Butler, J. E.; Ziegler, K. J. *J. Am. Chem. Soc.* **2008**, *130*, 14721.
- (18) Levy, R. M.; Zhang, L. Y.; Gallicchio, E.; Felts, A. K. *J. Am. Chem. Soc.* **2003**, *125*, 9523.
- (19) Martel, R.; Shea, H. R.; Avouris, P. *J. Phys. Chem. B* **1999**, *103*, 7551.
- (20) (a) Shen, J. M.; Liu, A. D.; Tu, Y.; Foo, G. S.; Yeo, C. B.; Chan-Park, M. B.; Jiang, R. R.; Chen, Y. *Energy Environ. Sci.* **2011**, *4*, 4220. (b) Yu, A. P.; Su, C. C. L.; Roes, I.; Fan, B.; Haddon, R. C. *Langmuir* **2010**, *26*, 1221.
- (21) Torza, S.; Mason, S. G. *J. Colloid Interface Sci.* **1970**, *33*, 67.
- (22) (a) Teng, X. W.; Han, W. Q.; Ku, W.; Hucker, M. *Angew. Chem., Int. Ed.* **2008**, *47*, 2055. (b) Wang, D. H.; Zhou, W. L.; McCaughy, B. F.; Hampsey, J. E.; Ji, X. L.; Jiang, Y. B.; Xu, H. F.; Tang, J. K.; Schmehl, R. H.; O'Connor, C.; Brinker, C. J.; Lu, Y. F. *Adv. Mater.* **2003**, *15*, 130.
- (23) Huang, X. Q.; Zheng, N. F. *J. Am. Chem. Soc.* **2009**, *131*, 4602.
- (24) (a) Lee, H. W.; Muralidharan, P.; Ruffo, R.; Mari, C. M.; Cui, Y.; Kim, D. K. *Nano Lett.* **2010**, *10*, 3852. (b) Wang, X.; Li, Y. D. *J. Am. Chem. Soc.* **2002**, *124*, 2880.
- (25) Zhu, L. F.; Wang, H.; Shen, X. S.; Chen, L. Y.; Wang, Y. W.; Chen, H. Y. *Small* **2012**, *8*, 1857.